

Report

Recruitment Collapse and Population Structure of the European Eel Shaped by Local Ocean Current Dynamics

Miguel Baltazar-Soares,^{1,*} Arne Biastoch,¹ Chris Harrod,^{2,3} Reinhold Hanel,⁴ Lasse Marohn,⁴ Enno Prigge,¹ Derek Evans,⁵ Kenneth Bodles,⁶ Erik Behrens,¹ Claus W. Böning,¹ and Christophe Eizaguirre^{1,2}

¹GEOMAR Helmholtz Centre for Ocean Research Kiel, Düsterbrooker Weg 20, 24105 Kiel, Germany

²School of Biological and Chemical Sciences, Queen Mary University of London, Mile End Road, London E1 4NS, UK

³Instituto de Ciencias Naturales Alexander Von Humboldt, Universidad de Antofagasta, Avenida Angamos 601, Antofagasta, Chile

⁴Thünen-Institute of Fisheries Ecology, Palmaille 9, 22767 Hamburg, Germany

⁵Fisheries and Aquatic Ecosystems Branch, Agri-Food and Biosciences Institute, Newforge Lane, Belfast BT9 5PX, UK

⁶School of Biological Sciences, Queen's University Belfast, 97 Lisburn Road, Belfast BT9 7BL, UK

Summary

Worldwide, exploited marine fish stocks are under threat of collapse [1]. Although the drivers behind such collapses are diverse, it is becoming evident that failure to consider evolutionary processes in fisheries management can have drastic consequences on a species' long-term viability [2]. The European eel (*Anguilla anguilla*; Linnaeus, 1758) is no exception: not only does the steep decline in recruitment observed in the 1980s [3, 4] remain largely unexplained, the punctual detection of genetic structure also raises questions regarding the existence of a single panmictic population [5–7]. With its extended Transatlantic dispersal, pinpointing the role of ocean dynamics is crucial to understand both the population structure and the widespread decline of this species. Hence, we combined dispersal simulations using a half century of high-resolution ocean model data with population genetics tools. We show that regional atmospherically driven ocean current variations in the Sargasso Sea were the major driver of the onset of the sharp decline in eel recruitment in the beginning of the 1980s. The simulations combined with genotyping of natural coastal eel populations furthermore suggest that unexpected evidence of coastal genetic differentiation is consistent with cryptic female philopatric behavior within the Sargasso Sea. Such results demonstrate the key constraint of the variable oceanic environment on the European eel population.

Results and Discussion

Oceanographic Modeling

We studied the effect of mesoscale currents and their variation on the European eel (*Anguilla anguilla*) over more than half a century using a novel high-resolution ocean model [8, 9], atmospherically driven with improved reanalysis products [10]. In silico, we released 8×10^6 virtual eels (v-eels) in an

area, depth, and time range reflecting the putative spawning area of the species [11, 12], allowing them to disperse [13] following realistic ocean conditions. This experiment was repeated annually for the period between 1960 and 2005. We subsequently defined v-eels as "successful" if they reached the continental shelf (25°W meridian) within a 2-year period within the simulation [14]. With this approach, we confirmed the existence of an ocean bifurcation pathway [15] that emerges only at sufficient spatial model resolution [16] and also a strong year-to-year variability in numbers at the European coastlines [17] (Figure 1). The north branch of the ocean bifurcation reflects the presence of European eel at high latitudes; the southern branch suggests the presence of eel larvae around the Canary Islands and Madeira, a prediction supported by field data [18]. The confirmation of such results provides an important demonstration of the resolution power of our novel model.

Owing to the extended period over which our model iterated variation in oceanic conditions, we were able to investigate the relative role of interannual to decadal oceanic variability on the eel recruitment: particularly, when comparing recruitment prediction from v-eels with actual observed recruitment available in International Council for the Exploration of the Seas (ICES) reports, the ocean model was strong in predicting both annual fluctuations and the collapse of observed recruitment ($F_{VR} \times \text{time} = 35.08$; $p < 0.001$; Figure 2). Interestingly, the significant interaction in our statistical linear model between v-eels and the period (before/after) of the major recruitment collapse shows that the correlation between oceanic fluctuations and eel recruitment was lost. Such significant interaction suggests that the lack of recovery in the European eel recruitment after the notorious decline was associated with other exogenous pressures such as parasites, pollutants, and/or lack of spawners [19–22]. Nonetheless, our study gives conclusive evidence for an oceanographic onset of the recruitment decline of the European eels.

Our analyses also revealed that years showing high dispersal rates were characterized by predominantly westward currents in the variable flow regime east of the Bahamas [23], providing a "shortcut" of the much longer route to the Gulf Stream through the Caribbean Sea. In those years, a large fraction of the v-eels can reach the Gulf Stream in a matter of weeks (Figure 1). In years with lower dispersal rates, the shortcut was absent, so that v-eels could only follow the extended migration route through the Caribbean Sea. We identified that the existence of the shortcut is dependent on the regional wind characteristics shaping the details of the western part of the subtropical gyre (see Figure S1 available online). Note that the general spreading pattern is not significantly affected by depth of v-eel release (e.g., 300 m) or longer dispersal periods (e.g., 3 years) (data not shown).

The spatial and temporal variability of the currents observed in the Sargasso Sea revealed that the spawning ground of the European eel was highly dynamic and that such variation strongly affected eel recruitment (Figure S1). What, then, are the consequences of such heterogeneous environments on genetic structure in coastal Western European eel populations? This question is important because conflicting reports

*Correspondence: msoares@geomar.de

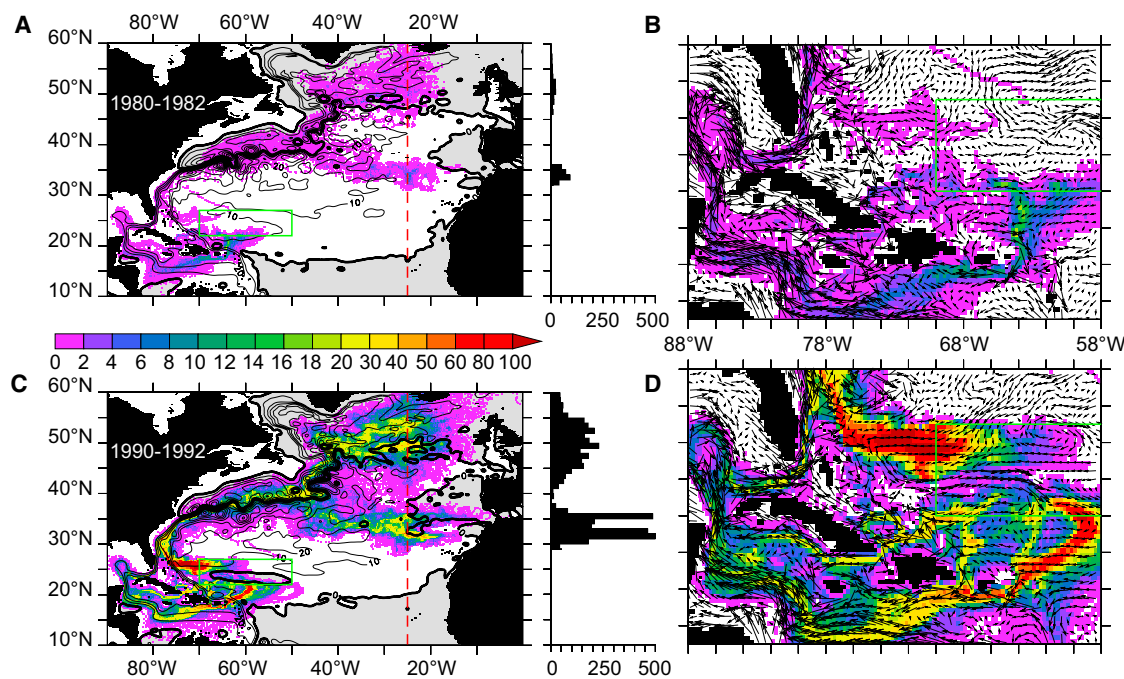


Figure 1. Simulated v-Eel Dispersal Rates

(A and C) Examples of low (A; 1980–1982) and high (C; 1990–1992) dispersal rates ($\text{in } 10^{-2} \text{ eels/m}^2$) from the released area (50°W – 70°W ; 22°N – 27°N) in the Sargasso Sea (green box) toward 25°W within 2 years. Oceanic circulation is contoured by the horizontal stream function (1-year average). Histograms show the number of v-eels arriving at 25°W , binned at 1° resolution and summed over the first 100 m of the water column.

(B and D) Close-up of dispersal rates and ocean currents, averaged over the first 3 months after release for low and high years.

regarding the existence of a panmictic breeding system in eels have raised questions regarding the existence of a single, randomly mating population. Such conclusions have also important implications for conservation and fisheries management, as numerous early-life-stage eels are translocated among watersheds in order to support fisheries, possibly affecting sensory cues required to return to the Sargasso Sea [18, 24].

In Silico Population Genetics

We first examined this question in silico by (1) generating two genetically distinct spawning scenarios—panmixia versus female philopatry (Figure S2)—within the high-resolution ocean circulation models and (2) comparing genetic signatures of artificially created populations at the 25°W meridian. Overall analysis showed that under the scenario of panmixia, no spatial or temporal genetic structure was detectable on European coasts (analysis of molecular variance [AMOVA]; 99% of overall variation within all populations; $p < 0.001$). Conversely, the scenario of female philopatry constrained the distribution of both spatial (among sites within years = 1.2% of overall variability, $p < 0.01$) and temporal (among release events = 8.6% of overall variation, $p < 0.001$; within continental sites, among release events = 9.8% of overall variation, $p < 0.001$) genetic variability in European populations (Tables S1A and S1B).

In spite of a homogenizing effect of the ocean, the overall degree of in silico estimated F_{ST} differentiation was higher under the female philopatry scenario than under panmixia (panmixia $F_{ST} = 0.01 \pm 0.006$ [SEM]; female philopatry $F_{ST} = 0.03 \pm 0.01$; $t = 2.14$, $df = 12.65$, $p = 0.05$). Interestingly, spatial pairwise comparisons among continental v-eel populations (Table S2) revealed that observable genetic structure can result from both the panmixia and female philopatry scenarios, especially

in years of low recruitment. Those structures were not linked to any obvious form of isolation by distance (all Mantel tests $p > 0.001$; Table S3). Pairwise comparisons (Table S2) of modeled genetic structure across different temporal periods also revealed significantly higher genetic differentiation under female philopatry than under panmixia (Student's test; $t = 5.49$, $df = 7.26$, $p < 0.0001$), suggesting that a nonpanmictic mode of evolution may result in an isolation by time [6]. Considered together, our results unify previous conflicting reports regarding the evidence for a panmictic mode of reproduction in European eels, as even under this mode of evolution, under low recruitment conditions, departure from signature of random mating can exist on European coasts [6, 7, 25]. Our model outputs provided support for the hypothesis that the genetic signature of spatially structured (or even panmictic) distribution within the Sargasso Sea should be reflected as observable genetic structure in eels recruiting to European coastal populations.

Because the relative number of successfully arriving v-eels produced by each event was negatively correlated with the mean F_{ST} values associated with the female philopatry scenario (Spearman rank correlation: $\rho = -0.69$, $p = 0.04$), we predict that any observed genetic structure will be stronger under conditions of low recruitment. No such relationship was observed under the scenario of panmixia (Figure S2).

Molecular Analyses of Natural Populations

After our in silico examination of the role of different modes of reproduction in v-eel populations, we tested for signatures of genetic structure in natura based on the hypotheses emitted from the ocean current models. Hence, we sampled yellow-phase eels from contemporary populations from 13 different

A. *anguilla* Life History Shaped by Ocean Currents

3

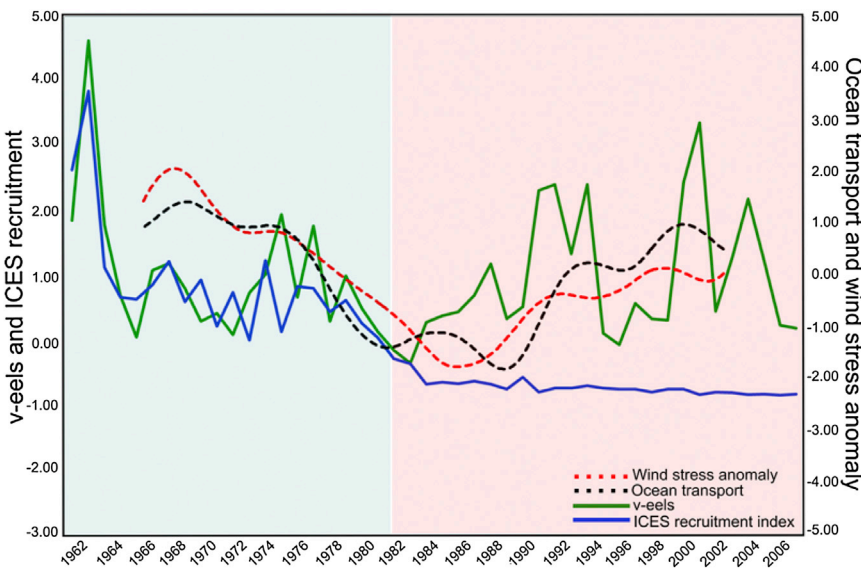


Figure 2. Natural Recruitment, Simulated Virtual Recruitment, and Wind Forcing between 1962 and 2007

Left y axis: ICES-NS natural recruitment index (blue curve) and virtual recruitment (v-eels, green curve). Right y axis: ocean transport (dashed black line) at 70°W, integrated between 24°N and 27°N. The wind stress anomaly (dashed red line) was integrated between 24°N and 28°N and between 60°W and 50°W (values were multiplied by -1 for representation purposes). For transport and wind stress, a 121-month Hanning filter was applied to focus on decadal timescales.

sites located along the natural marine-freshwater salinity gradient inhabited by this species [26]. This strategy was devised to screen variation across both large and small geographic scales. We assessed polymorphism of the *ND5* region of the mitochondrial genome (which should best reflect female-mediated structure such as philopatry) as well as 17 nuclear loci (which should provide a more contemporary picture of mating systems). Information on natural populations can be found in Table S5. Consistent with some of the previous findings using nuclear markers [5, 6], we found weak but significant genetic structure among some sampling locations (Table S6). More striking however, was the strong and significant genetic structure detected using the maternally inherited mtDNA (Figure 3A; Table S6), which was significantly higher than that shown using nuclear markers (mtDNA $F_{ST} = 0.11 \pm 0.002$ [SEM]; microsatellites $F_{ST} = 0.02 \pm 0.0001$; $t = 7.96$, $df = 9$, $p < 0.001$). Although this pattern may arise from slower allelic fixation of microsatellites and a 4-fold higher effective population size of nuclear DNA (nDNA) compared to mtDNA [27], lower levels of nuclear differentiation are generally thought to arise from female structured populations and male-mediated gene flow through opportunistic mating [28]. Deeper investigations on mtDNA gene phylogeny showed multiple lines of evidence supporting the existence of subpopulations at the source location (Figures 3B and S3; Tables S5, S6, and S7).

Importantly, the overall order of magnitude of F_{ST} detected via mtDNA sequencing reflected the higher F_{ST} levels predicted from our in silico scenario simulating female philopatry. This correlation and the maternal inheritance of mtDNA [29] suggest the discovery of a previously unreported mode of reproductive behavior in the European eel, where females are philopatric to and within locations in the Sargasso Sea, whereas males maintain gene flow by returning earlier than females to the spawning ground where they may mate opportunistically [18, 30]. Although the mechanisms underlying the homing behavior in this species are not well understood [31] and may be linked to the Earth's magnetic field [24], life history strategies of this kind are common both in aquatic and terrestrial organisms [28, 32].

In summary, a process of atmospherically driven dispersal by ocean currents connects the putative spawning grounds of the European eel and the Gulf Stream, greatly enhancing

the arrival of juveniles at the European coast. When atmospheric-oceanographic conditions shift and this mechanism is absent, eel recruitment is low, explaining the onset of the large-scale collapse in recruitment that occurred during the 1980s. Following

the crash, the capacity of the eel population to recover not only was limited by a reduced supply of potential recruits but was further diminished by the effects of a multitude of anthropogenic impacts, combining to limit the probability of recovery of this ecologically and economically important species. To compensate for the shortage of eels in European freshwater systems, management measures such as stocking of eels across large geographical scales have been put in place. The assumption of a panmictic breeding system was thought to limit any consequences of such movement of individuals, but our work suggests that this may have unexpected impacts and furthermore may affect the recovery of this species. Finally, our work highlights the potential power of combining oceanographic modeling with modern population genetics, and the fusion of the two approaches will likely represent a valuable tool to understand the fundamental basis of species' evolutionary biology and ultimately optimize conservation programs.

Experimental Procedures

Oceanographic Modeling

We investigated the effects of oceanographic variability along the known dispersal pathway connecting the European eel's spawning grounds (Sargasso Sea) and the European coast by utilizing a global ocean circulation model with a very high resolution ($1/20^{\circ}$, ~4 to 5 km grid size) in the North Atlantic between 32°N and 85°N (VIKING20), accomplished by a two-way nesting approach [8] into the ORCA025 model [33] based on the NEMO code [9]. Owing to its very high resolution, which was identified as an important prerequisite for a realistic simulation of eel dispersal [16], advanced numerics [34], and a synoptic atmospheric forcing of the period 1948–2007 [10], our model allows the investigation of spatiotemporal variability of oceanic circulation influences with much improved verisimilitude. A detailed description of the VIKING20 ocean model is provided in the *Supplemental Experimental Procedures* and Figure S4. In short, using a Lagrangian tracking technique [13], we released 8×10^6 virtual eels (v-eels) in an area and depth range reflecting the putative spawning area of the European eel [11, 12], following results and discussion for vertical distribution in [14]. Release was performed during the month of May (from the 1st until the 31st) [35]. We then calculated the dispersion of the v-eels with the transient three-dimensional flow field of the base model. The procedure was repeated for every year during the 1960–2005 period. Particles reaching the eastern North Atlantic (25°W) within 2 years of advection were defined as successful migrants [14] and entered subsequent recruitment and genetic analyses.

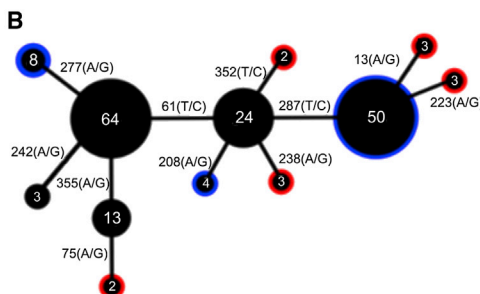
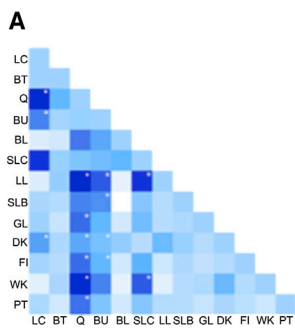


Figure 3. Observed Genetic Differentiation and Phylogeny in the mtDNA Gene

(A) mtDNA pairwise comparison matrix among 13 eel populations here represented as a heatmap (Arlequin v3.5 R graphical interface). White asterisks identify pairwise locations shown to differ significantly in haplotype composition. Significant F_{ST} values ranged between 0.058 (Q/DK) and 0.16 (Q/LL).

(B) Phylogeny and haplotype relationships are shown here in the format of a simplified haplotype network (no unique haplotypes). Numbers inside each haplotype represent that haplotype's frequency; branching numbers represent polymorphism defining the haplotypes. Red and blue markers reflect the neighbor-joining tree; blue = 50 < bootstrap < 60; red = 60 < bootstrap.

Virtual and Natural Recruitment

The hypothesis that ocean currents drive European eel recruitment and decline was tested by the statistical comparison of natural [36] and virtual recruitment. The recruitment data set used in this study corresponded to generalized linear model of recruitment for the North Sea, hereafter referred as "ICES," as it incorporates the longest recruitment index for the European eel, Den Oever [36]. Both types of recruitment were standardized to their z scores for direct comparisons. For statistical purposes, we defined "decline" as the time point where natural recruitment z scores became consistently negative; the factor "time" was introduced to delimit the periods "before" and "after" the population collapse. The relationship between natural and virtual recruitment before and after the decline was inferred by linear models run in R [37]. Ocean transport and wind forcing were also standardized to their z scores.

In Silico Population Genetics

We integrated the eel genetic component to the oceanic model by splitting the released particles into ten different mtDNA haplotypes. These haplotypes were distributed either randomly or along ten subareas within the Sargasso Sea. Here, we aimed to simulate the consequences on eel distribution at continental sites of a panmictic spawning ground versus a contrasting scenario of complete genetic structure which would correspond to the population signature of female philopatry within the spawning ground. Subsequently, successfully arriving (i.e., within the 2-year period) v-eels were split, on the European coast, into an equal amount of ten populations—each population spanning 4° latitude (Figure S2). To discriminate any effects of temporally and spatially isolated samplings on genetic structure under both spawning scenarios, we performed two AMOVAs: (1) among release events and (2) among artificial populations at continental sites. The capacity of the release events to generate genetic structure at the coast was also examined by calculating Wright's index (F_{ST}) pairwise comparisons among artificial populations. Isolation by distance was calculated among artificial populations. To this end, geographical distances were converted according to the relation 1° latitude = 110 km. Finally, to investigate the possible link between recruitment and population structure at continental sites under the proposed spawning scenarios, we correlated each release event's averaged F_{ST} with the proportion (Table S1) of successfully arriving particles.

Molecular Analyses and Populations Genetics

The presence of genetic structure among European eel coastal locations was evaluated by sampling yellow eels spanning 13 locations (Table S2A) across both small (within Ireland) and large (additional four continental sites) geographical scales. A total of 240 individuals were examined for a section of the ND5 (355 bp) mitochondrial gene as well as 17 nuclear loci. Population structure was accessed through calculation of F_{ST} values between populations. We also added eight American eel (*A. rostrata*) sequences to test for neutral evolution of the mitochondrial marker. Detailed descriptions of molecular protocols, analyses, and software used are given in the Supplemental Experimental Procedures.

Supplemental Information

Supplemental Information includes four figures, seven tables, and Supplemental Experimental Procedures and can be found with this article online at <http://dx.doi.org/10.1016/j.cub.2013.11.031>.

Acknowledgments

The authors would like to thank A. Hasselmeyer, G. Ramm, and Y. Sakai for laboratory assistance; D. Cairns for *A. rostrata* samples; and J. Duhart for sharing *A. anguilla* samples. C.H., D.E., and K.B. thank the Department of Culture Art and Leisure (NI), which supports all eel research in Northern Ireland, and R. Poole of the Marine Institute, Westport, Ireland. K.B. is funded by the Department of Employment and Learning (NI). M.B.-S. is funded by the International Max Planck Research School for Evolutionary Biology. This work was funded partly by a Leibniz Institute competitive grant and Deutsche Forschungsgemeinschaft grants to C.E. (El 841/4-1 and El 841/6-1). The development of the ocean model received funding from the European Union's Seventh Framework Programme (FP7/2007-2013) under grant agreement number 212643 (EU-THOR). The model integrations were performed at the North-German Supercomputing Alliance (HLRN). The DNA haplotype sequences can be found in Data Set S1.

Received: June 6, 2013

Revised: September 24, 2013

Accepted: November 15, 2013

Published: December 26, 2013

References

- Costello, C., Ovando, D., Hilborn, R., Gaines, S.D., Deschenes, O., and Lester, S.E. (2012). Status and solutions for the world's unassessed fisheries. *Science* 338, 517–520.
- Conover, D.O., and Munch, S.B. (2002). Sustaining fisheries yields over evolutionary time scales. *Science* 297, 94–96.
- Moriarty, C. (1990). European catches of elver of 1928–1988. *Int. Rev. Gesamten Hydrobiol. Hydrogr.* 75, 701–706.
- Dekker, W. (2000). The fractal geometry of the European eel stock. *ICES J. Mar. Sci.* 57, 109–121.
- Wirth, T., and Bernatchez, L. (2001). Genetic evidence against panmixia in the European eel. *Nature* 409, 1037–1040.
- Dannevitz, J., Maes, G.E., Johansson, L., Wickström, H., Volckaert, F.A.M., and Järvi, T. (2005). Panmixia in the European eel: a matter of time. *Proc. Biol. Sci.* 272, 1129–1137.
- Als, T.D., Hansen, M.M., Maes, G.E., Castonguay, M., Riemann, L., Aarestrup, K.I.M., Munk, P., Sparholt, H., Hanel, R., and Bernatchez, L. (2011). All roads lead to home: panmixia of European eel in the Sargasso Sea. *Mol. Ecol.* 20, 1333–1346.
- Debrey, L., Vouland, C., and Blayo, E. (2008). AGRIF: Adaptive grid refinement in Fortran. *Comput. Geosci.* 34, 8–13.
- Madec, G.; NEMO Team (2008). NEMO ocean engine, Note du Pôle de modélisation (Paris: Institut Pierre-Simon Laplace).
- Large, W.G., and Yeager, S.G. (2009). The global climatology of an inter-annually varying air-sea flux data set. *Clim. Dyn.* 33, 341–364.
- McCleave, J.D., Kleckner, R.C., and Castonguay, M. (1987). Reproductive sympatry of American and European eels and implications for migration and taxonomy. In *American Fisheries Society Symposium, Volume 1* (Bethesda: American Fisheries Society), pp. 286–297.
- Castonguay, M., and McCleave, J.D. (1987). Vertical distributions, diel and ontogenetic vertical migrations and net avoidance of leptocephali of *anguilla* and other common species in the Sargasso Sea. *J. Plankton Res.* 9, 195–214.

A. anguilla Life History Shaped by Ocean Currents

5

13. Blanke, B., Arhan, M., Madec, G., and Roche, S. (1999). Warm water paths in the equatorial Atlantic as diagnosed with a general circulation model. *J. Phys. Oceanogr.* **29**, 2753–2768.
14. Bonhommeau, S., Chassot, E., and Rivot, E. (2008). Fluctuations in European eel (*Anguilla anguilla*) recruitment resulting from environmental changes in the Sargasso Sea. *Fish. Oceanogr.* **17**, 32–44.
15. Bonhommeau, S., Blanke, B., Tréguier, A.-M., Grima, N., Rivot, E., Vermaud, Y., Greiner, E., and Le Pape, O. (2009). How fast can the European eel (*Anguilla anguilla*) larvae cross the Atlantic Ocean? *Fish. Oceanogr.* **18**, 371–385.
16. Blanke, B., Bonhommeau, S., Grima, N., and Drillet, Y. (2012). Sensitivity of advective transfer times across the North Atlantic Ocean to the temporal and spatial resolution of model velocity data: Implication for European eel larval transport. *Dyn. Atmos. Oceans* **55–56**, 22–44.
17. Kettle, A.J., Bakker, D.C.E., and Haines, K. (2008). Impact of the North Atlantic Oscillation on the trans-Atlantic migrations of the European eel (*Anguilla anguilla*). *J. Geophys. Res.* **113**, G03004.
18. Tesch, F. (2003). *The Eel* (Oxford: Blackwell Sciences).
19. Feunteun, E. (2002). Management and restoration of European eel population (*Anguilla anguilla*): An impossible bargain. *Ecol. Eng.* **18**, 575–591.
20. Dekker, W. (2003). Did lack of spawners cause the collapse of the European eel, *Anguilla anguilla*? *Fish. Manage. Ecol.* **10**, 365–376.
21. Palstra, A.P., van Ginneken, V.J., Murk, A.J., and van den Thillart, G.E. (2006). Are dioxin-like contaminants responsible for the eel (*Anguilla anguilla*) drama? *Naturwissenschaften* **93**, 145–148.
22. Palstra, A.P., Heppener, D.F.M., van Ginneken, V.J.T., Székely, C., and van den Thillart, G.E.E.J.M. (2007). Swimming performance of silver eels is severely impaired by the swim-bladder parasite *Anguillicola crassus*. *J. Exp. Mar. Biol. Ecol.* **352**, 244–256.
23. Frajka-Williams, E., Johns, W.E., Meinen, C.S., Beal, L.M., and Cunningham, S.A. (2013). Eddy impacts on the Florida Current. *Geophys. Res. Lett.* **40**, 349–353.
24. Durif, C.M.F., Browman, H.I., Phillips, J.B., Skiftesvik, A.B., Vøllestad, L.A., and Stockhausen, H.H. (2013). Magnetic compass orientation in the European eel. *PLoS ONE* **8**, e59212.
25. Palm, S., Dannewitz, J., Prestegaard, T., and Wickström, H. (2009). Panmixia in European eel revisited: no genetic difference between maturing adults from southern and northern Europe. *Heredity (Edinb)* **103**, 82–89.
26. Harrod, C., Grey, J., McCarthy, T.K., and Morrissey, M. (2005). Stable isotope analyses provide new insights into ecological plasticity in a mixohaline population of European eel. *Oecologia* **144**, 673–683.
27. Avise, J.C., Bowen, B.W., Lamb, T., Meylan, A.B., and Bermingham, E. (1992). Mitochondrial DNA evolution at a turtle's pace: evidence for low genetic variability and reduced microevolutionary rate in the Testudines. *Mol. Biol. Evol.* **9**, 457–473.
28. Bowen, B.W., Bass, A.L., Chow, S.-M., Bostrom, M., Bjorndal, K.A., Bolten, A.B., Okuyama, T., Bolker, B.M., Epperly, S., Lacasella, E., et al. (2004). Natal homing in juvenile loggerhead turtles (*Caretta caretta*). *Mol. Ecol.* **13**, 3797–3808.
29. Birky, C.W., Jr. (2001). The inheritance of genes in mitochondria and chloroplasts: laws, mechanisms, and models. *Annu. Rev. Genet.* **35**, 125–148.
30. Dou, S.Z., Yamada, Y., Okamura, A., Tanaka, S., Shinoda, A., and Tsukamoto, K. (2007). Observations on the spawning behavior of artificially matured Japanese eels *Anguilla japonica* in captivity. *Aquaculture* **266**, 117–129.
31. Wirth, T., and Bernatchez, L. (2003). Decline of North Atlantic eels: a fatal synergy? *Proc. Biol. Sci.* **270**, 681–688.
32. Brower, L. (1996). Monarch butterfly orientation: missing pieces of a magnificent puzzle. *J. Exp. Biol.* **199**, 93–103.
33. Behrens, E., Biastoch, A., and Böning, C.W. (2013). Spurious AMOC trends in global ocean sea-ice models related to subarctic freshwater forcing. *Ocean Model.* **69**, 39–49.
34. Barnier, B., Madec, G., Penduff, T., Molines, J.-M., Treguier, A.-M., Le Sommer, J., Beckmann, A., Biastoch, A., Böning, C., Dengg, J., et al. (2006). Impact of partial steps and momentum advection schemes in a global ocean circulation model at eddy-permitting resolution. *Ocean Dyn.* **56**, 543–567.
35. Castonguay, M. (1987). Growth of American and European eel leptocephali as revealed by otolith microstructure. *Can. J. Zool.* **65**, 875–878.
36. ICES (2011). Report of the Joint EIFAC/ICES Working Group on Eels (WGEEL), September 5–9, 2011, Lisbon, Portugal (Lisbon: International Council for the Exploration of the Seas).
37. Fox, J. (2005). The R commander: A basic statistics graphical user interface to R. *J. Stat. Softw.* **14**, 1–42.

Supplemental Information

Recruitment Collapse and Population

Structure of the European Eel

Shaped by Local Ocean Current Dynamics

Miguel Baltazar-Soares, Arne Biastoch, Chris Harrod, Reinhold Hanel, Lasse Marohn, Enno Prigge, Derek Evans, Kenneth Bodles, Erik Behrens, Claus W. Böning, and Christophe Eizaguirre

Supplemental Figures

Figure S1. This figure has 4 panels. It relates to the association between oceanography and recruitment depicted in main figures 1 and 2, with a detailed description of the wind-ocean interaction.

Figure S2. This figure has 2 panels. These figures are a visual support for both methodology and results of the section “*In silico* population genetics” on main document.

Figure S3. This figure has 2 panels and presents deep phylogenetic analyses of the mitochondrial marker used in this study.

Figure S4. This figure has 3 panels. This additional information shows the validation of the ocean model used in this study. Results are compared with satellite and moored data.

Supplemental Tables

Table S1. Analyses of molecular variance (AMOVA) based on haplotype frequencies, performed on artificial v-eel populations.

Table S2. Test for population structure and isolation by time on in silico v-eel populations (see separate Excel file)

Table S3. Test for isolation by distance on in silico v-eel populations

Table S4. Relationship between ocean characteristics and artificial population genetics

Table S5. Ecological, geographical and molecular information of individuals sampled for the study (see separate Excel file)

Table S6. Population structure of natural populations: pairwise comparisons performed with mtDNA and microsatellite markers

Table S7. Test for neutral evolution of the mitochondrial marker

Supplemental Experimental Procedures

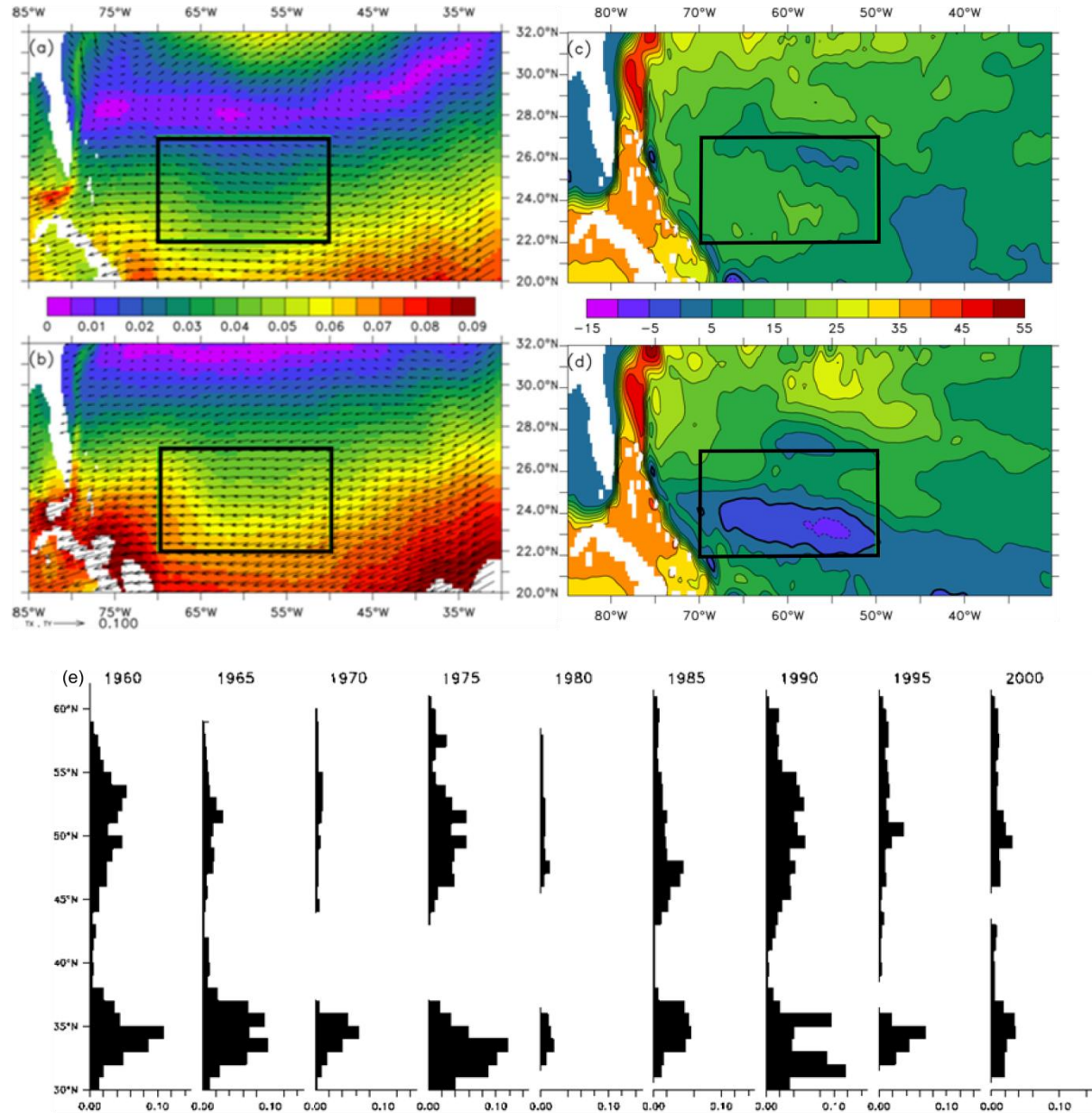
Text S1. Complements methodology of molecular analyses on natural populations

Supplemental References

Procedures and software cited in Supplemental Information

Supplemental Figures

Figure S1 - Influence of Oceanic Currents on the Eel Dispersal

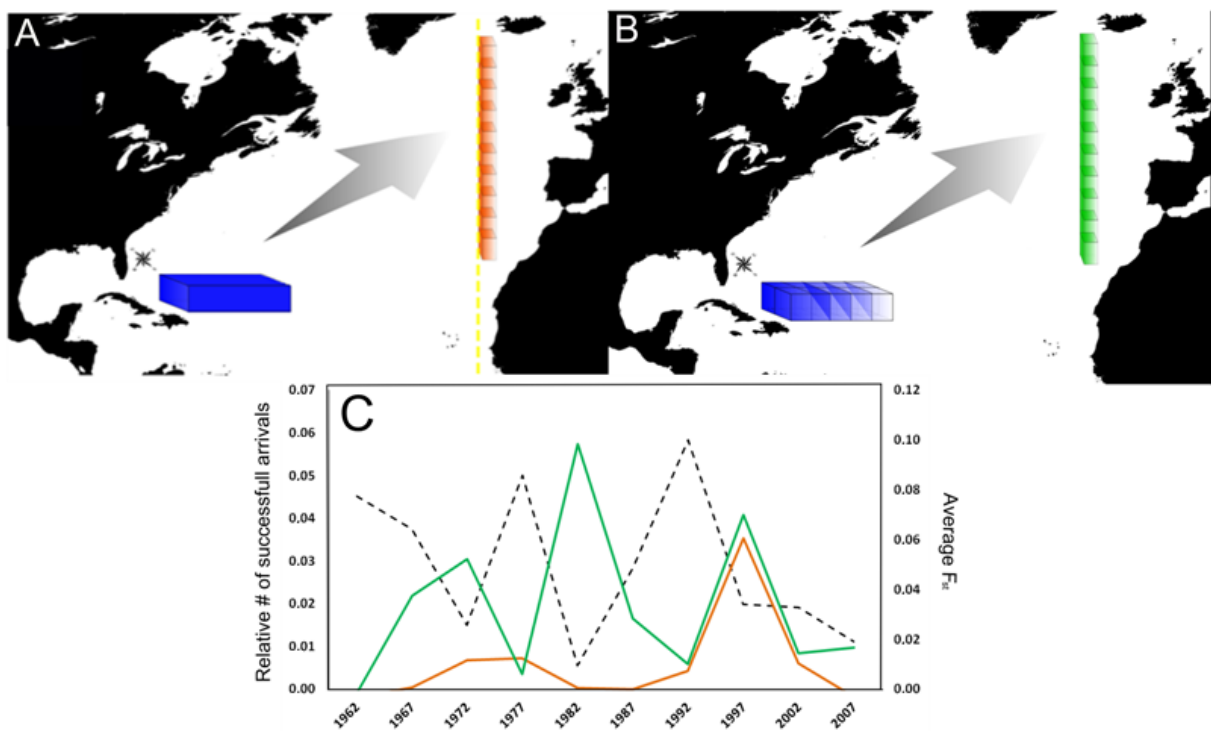


Atmospheric conditions and oceanic response in the vicinity of the v-eel release. Exemplarily v-eels for years of high (1990, a and c) and low (1980, b and d) dispersal. Shown are (a, b) magnitudes (in N/m^2) and vectors of wind stress and (c, d) the streamfunction (in Sv) of the horizontal gyre circulation. Positive values represent an anticyclonic (clockwise) circulation, with strong gradients indicating strong flows. The box of the v-eel release is indicated in black. **Panel e:** Cumulated proportions of v-eels successfully arriving at $25^\circ W$, binned at 1° -resolution and summed up over the first 100 meters of the water column. Examples are given for 9 temporal simulations (every 5 years but simulations were run yearly). The numerical representation of the year corresponds to the beginning of simulation period. The particles were allowed to disperse for 2 years.

Atmospheric winds are one of the main drivers for the oceanic current variability. The large-scale wind pattern in the subtropical North Atlantic shapes the structure of the subtropical gyre, leading to prevailing westward but weak currents around $20^\circ N$. Crucial for the shortcut between the Sargasso Sea towards the Gulf Stream is the highly variable Antilles Current. Anomalous southward positions of the high-pressure systems (e.g., in the year

1980, Fig. S1b) lead to a southward shift of the currents in the subtropical gyre (Fig. S1d), not capturing the region northwest of the Sargasso Sea. In contrast, years of strong trades (Fig. S1a) feature strong westward currents in the Sargasso Sea and allow the direct migration of v-eels via a shortcut (see main document) towards the Gulf Stream. In addition, the upper ocean is subject to a direct influence from the local wind, the ‘Ekman effect’ that modulates currents with an angle between $\sim 20^\circ$ and 90° [S1] to the right in the top 50 m of the water column. Wind systems like the one in year 1990 (Fig. S1b) additionally favor northwestward currents in the upper layers [S2].

Figure S2 - *In silico* population genetics



Panel A and B: Schematic representation of the simulation procedure undertaken to access the effects of a panmictic (A-left, blue polygon) and philopatric (B-right, blue sectioned polygon) spawning grounds in the distribution of genetic variability at continental locations -orange and green-shaded cubes. The yellow line, drawn at 25 W meridian, defines the “successfully” arriving v-eels used for further analyses. **Panel C:** Correlation between the relative number of successful arrivals (black line, left Y-axis) and F_{ST} values associated with each spawning scenario (colored line, right Y-axis) for each release event (X-axis). Orange stands for the panmixia scenario and green for female philopatry. Spearman rank correlations and p-value between v-eel recruitment and F_{ST} are, respectively, $\rho_{\text{panmixia}} = 0.15$, p-value=0.69 ; $\rho_{\text{philopatry}} = -0.68$; p-value=0.04. Under the suspected mode of female philopatry reproductive strategy, years of low recruitment increase possibility for genetic structure, while only one simulated event (1997) would lead to significant F_{ST} under the panmictic mode of reproduction and no overall correlation with the simulated recruitment is observed.

Under the panmictic mode of reproduction, we created 10 genetic types (i.e. haplotypes) of unknown sequence. For each genetic type, 800 000 particles were released in the theoretical spawning ground randomly – thus reaching a total of 8 million v-eels to be tracked for 2 years. For the structured mode of evolution, the spawning ground was split into 10 regions, each consisting of one haplotype. 800 000 particles were released in each of the 10 regions reaching 8 million v-eels to also be tracked for 2 years. In both cases, v-eels were released in an area and depth range reflecting the putative spawning area of the European eel [S3,S4], following results and discussion for vertical distribution [S5]. Those parameters were chosen in order to allow comparison with previous studies but also to restrict already demanding simulations when possible. Varying depth of release and tracking period did not affect the overall described patterns for the tested simulations.

Figure S3 - Intraspecific phylogeny of natural populations

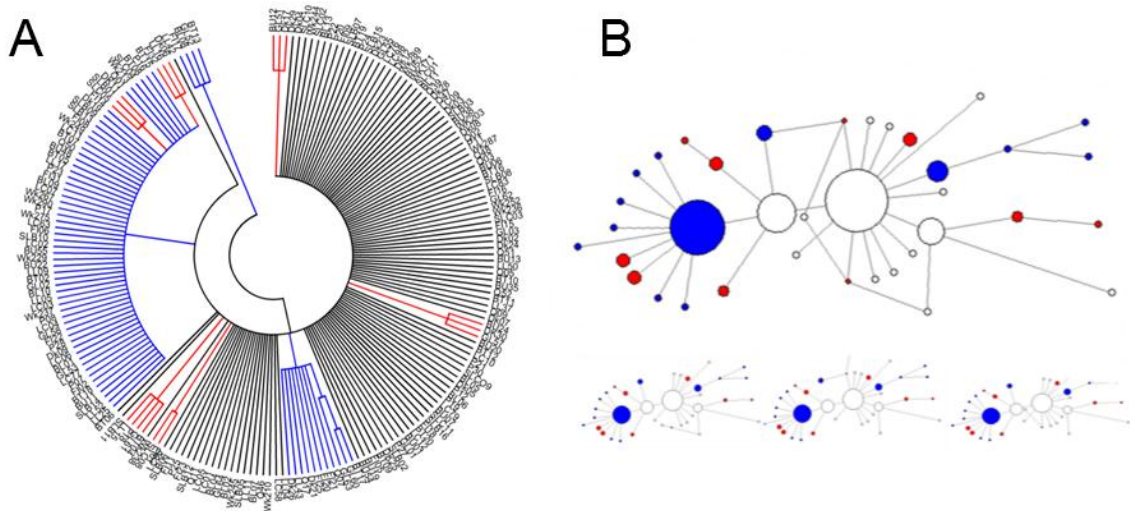
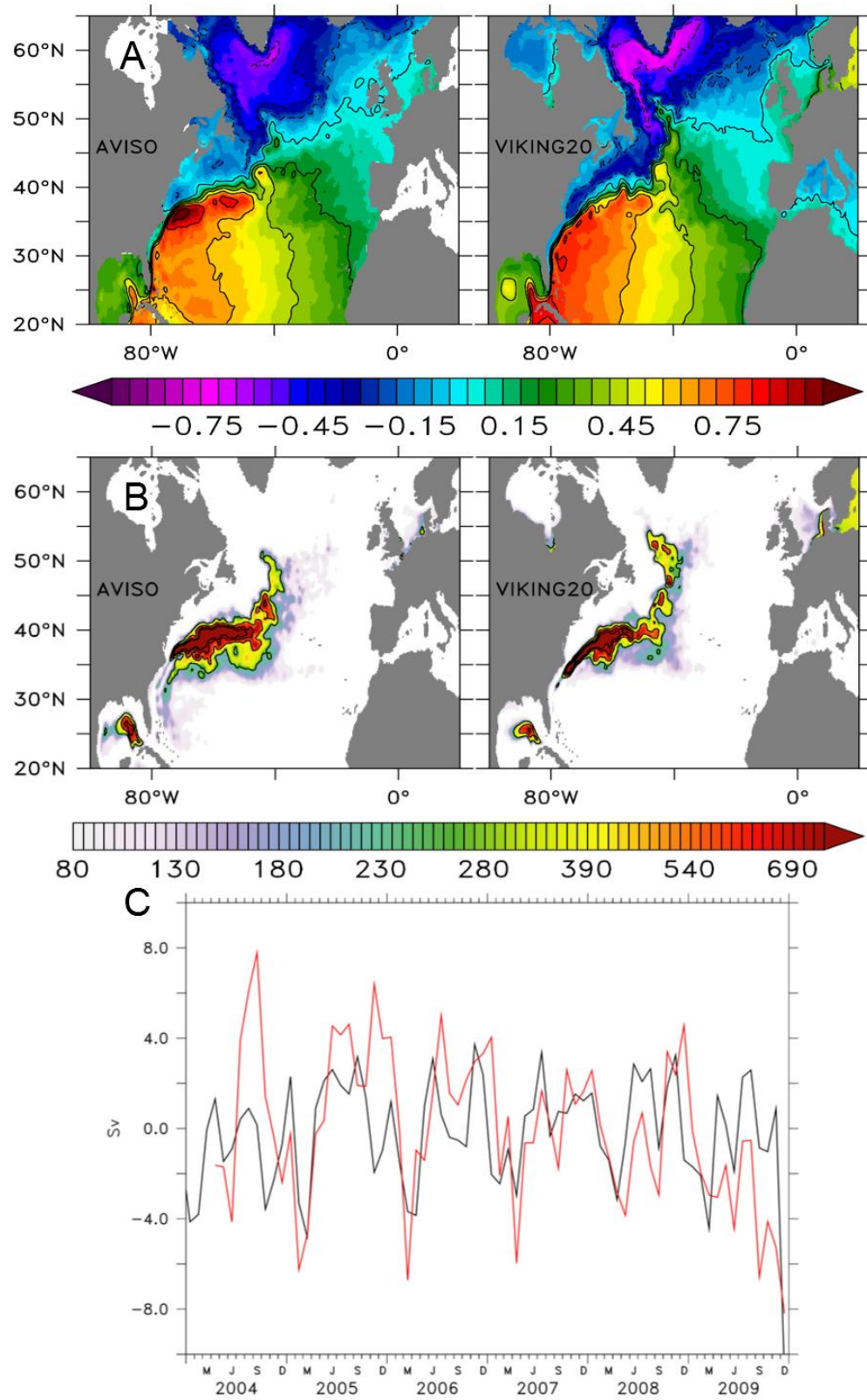


Figure S3 Phylogenetic tree (panel a) and haplotype networks (panel b) – We sampled yellow eels spanning 13 locations (Table S1), across both small (within Ireland) and large geographical (4 continental sites) scales. A total of 202 individuals were examined for a section of the *ND5* mitochondrial gene (355bp). The evolutionary history among sequences was inferred using the Neighbor-Joining method with 500 replications [S6]. The optimal tree with the sum of branch length = 0.109 is shown. The evolutionary distances were computed using the Maximum Composite Likelihood method [S7] and are given in number of base substitutions per site. The tree was condensed to show only bootstrap values >50, where branches in blue = 50<bootstrap<60 and in red = 60>bootstrap. **Haplotype networks (panel b).** Median joining network: every circle represents a detected haplotype. Size differences represent frequency in the overall samples. Filled haplotypes represent the group of individuals comprised in branches of the Neighbor-Joining tree, with same color. Red diamond-shaped forms depict median vectors. Also represented are the shortest trees generated by optimal post-processing (MP) maximum parsimony algorithm implemented in NETWORK v4.6.1.0 [S8]. The main network shows three major haplotypes - a pattern that clearly deviates from the star-like shape emerging from a single central haplotype characteristic of a panmictic population [S9]. This result suggests maternally mediated cryptic population structure.

Figure S4 - Characteristics of the VIKING20 ocean model



A - Mean sea-surface height (1998-2007, in m) for AVISO satellite (www.aviso.oceanobs.com) and VIKING20 model data. **B** - Variance of sea-surface height (1998-2007, in cm²) for AVISO (www.aviso.oceanobs.com) satellite and VIKING20 model data. **C** - Inter-annual variability of the meridional overturning strength (in Sv) in RAPID observations (red) and the VIKING20 model (black).

VIKING20 is a 1/20° model of the subtropical-subpolar North Atlantic (30°-80°N), nested into the 1/4° global ocean/sea-ice model (ORCA025). The oceanic currents and hydrography are simulated at great verisimilitude, both in mean and variability. Compared to satellite data, the model captures the path of the Gulf Stream and North Atlantic Current well, including the poleward turn into the Northwest Corner (panel **A**). The mesoscale representation (panel **B**) matches the correct level of variability and shows the two pathways of spreading towards Europe. The realism of interannual transport fluctuations is demonstrated by comparing the modelled transports at 26°N with observations from a moored RAPID array [S10] (panel **C**). Such ocean models, like HYCOM [S11] and NEMO [S12] accurately reproduce the trajectories of tracked drogues and so give a good representation of ocean flows. While the models may not reproduce every aspects of the real flows, they will give a good measure of flow variability and hence inter-annual patterns [S13]

Supplemental Tables

Table S1 – Population genetics on artificial populations: Analysis of molecular variance (AMOVA's) of artificial v-eel populations

Partitioning of genetic variation was inferred both across release events (**A**) and across artificial populations (**B**), assuming each spawning scenario (panmixia vs. philopatry). Only artificial populations that were supplied with more than 9 v-eels were taken into account in all further calculations.

Source of variation	A		d.f.		variation %		Φ statistic		p-value	
	Panmixia	Philopatry	Panmixia	Philopatry	Panmixia	Philopatry	Panmixia	Philopatry	Panmixia	Philopatry
Φct										
Among Years	9	9	-0.04	8.57	-0.0004	0.0857	0.29	<0.001		
Φsc										
Among sites within years	53	53	0.3	1.16	0.003	0.0127	<0.001	<0.001		
Φst										
Within Sites	12003	11443	99.74	90.27	0.0026	0.0973	<0.001	<0.001		
Source of variation	B		d.f.		variation %		Φ statistic		p-value	
	Panmixia	Philopatry	Panmixia	Philopatry	Panmixia	Philopatry	Panmixia	Philopatry	Panmixia	Philopatry
Φct										
Among Sites	5	6	-0.02	-1.14	-0.0002	-0.0114	0.33	0.87		
Φsc										
Among years within sites	52	55	0.25	9.84	0.0025	0.0973	<0.001	<0.001		
Φst										
Within Years	11893	11435	99.77	91.29	0.0023	0.0871	<0.001	<0.001		

A - AMOVA across release events considering data created by simulating panmixia and female philopatry ; “years” = release events, “sites” = artificial continental sites. **B** - AMOVA across artificial populations considering data created by simulating panmixia and female philopatry; “years” = release events, “sites” = artificial continental sites.

Table S2 – Pairwise comparisons of artificial populations (in excel format)

Table S3 – Isolation by distance between artificial populations

To test for isolation by distance amongst artificially created v-eel populations, we first converted latitudinal degrees into kilometers in the following website:

<http://www.ncgia.ucsb.edu/education/curricula/giscc/units/u014/tables/table01.html>

We applied Rousset's methods [S14] to calculate isolation-by-distance, i.e. log transformed geographic distances matrices and $F_{ST}/(1-F_{ST})$ transformed genetic distances matrices.

Release event		R ²	p-value
Panmixia			
1960-1962	y = -0.1146x+0.0334	0.0178	>0.05
1965-1967	y= 0.0791x -0.0243	0.0271	>0.05
1970-1972	y = 0.2250x-0.0625	8.81E+03	>0.05
1975-1977	y= 0.2826x -0.0808	2.16E+03	>0.05
1980-1982	y = -0.05346x+0.01735	0.0829	>0.05
1985-1987	y= 0.2339x -0.0642	0.0788	>0.05
1990-1992	y = 1.002x-0.2755	0.0428	>0.05
1995-1997	y= -0.1163x +0.0364	0.0432	>0.05
2000-2002	y = 0.0519x -0.0163	0.0168	>0.05
2005-2007	y= 0.1008x -0.0270	0.0405	>0.05
Female philopatry			
1960-1962	y = 0.6641x -0.1828	0.6563	>0.05
1965-1967	y= 0.2740x -0.0810	0.0768	>0.05
1970-1972	y = 1.298x -0.3691	0.029	>0.05
1975-1977	y= 0.6641x -0.1828	0.6563	>0.05

1980-1982	$y = 0.6160x - 0.1748$	0.8194	>0.05
1985-1987	$y = 1.266x - 0.3442$	0.0538	>0.05
1990-1992	$y = -1.988x + 0.6125$	0.154	0.05
1995-1997	$y = 0.1432x - 0.0391$	0.8166	>0.05
2000-2002	$y = -0.6037x + 0.1864$	0.0664	>0.05
2005-2007	$y = -0.2515x + 0.0796$	0.0282	>0.05

Mantel test between transformed F_{ST} -values based haplotype frequencies produced by each release event, assuming **panmixia** and **female philopatry**. Equations shows the linear regression between the two matrices used for the Mantel test: pairwise genetic and geographic distances.

Table S4 – Relationship between ocean currents and artificial population genetics

Years	Relative proportion of successful v-eels	Relative proportion of successful v-eels	
		North	South
1960	0.045	0.020	0.025
1965	0.037	0.008	0.029
1970	0.015	0.003	0.012
1975	0.050	0.020	0.030
1980	0.005	0.002	0.003
1985	0.028	0.014	0.015
1990	0.058	0.029	0.029
1995	0.020	0.009	0.010
2000	0.019	0.009	0.010
2005	0.011	0.004	0.007

Relative (in relation to 8×10^6 released v-eels) number of successful arriving v-eels at 25° W produced by each release event. Also relative numbers of successful arriving v-eels after the Mid Atlantic Ocean bifurcation: "North" and "South" were defined at 25° W by a perpendicular line superimposed in the 40° N meridian.

Table S5 – Additional information on natural populations (in excel format)

Table S6 – Pairwise comparisons amongst natural populations

Locations	LarneLagoon	Toome	Quoile	Burrihole	BannLower	Lough Comber	Larne Lough	Boretree	GlynnLagoon	Denmark	Finland	Germany	Portugal
LarneLagoon	-	0.003	0.007	0.009	0.019*	0.003	0.007	0.004	-0.001	-0.001	0.005	0.000	0.000
Toome	0.002	-	0.009	0.010*	0.023**	0.003	0.005	0.007	-0.002	0.003	0.005	0.002	-0.003
Quoile	0.150*	0.043	-	0.008	0.015*	0.009	0.005	0.013*	0.006	0.006	-0.001	0.006	0.004
Burrihole	0.096*	0.014	0.030	-	0.018*	0.005	0.007	0.002	0.002	0.004	0.008	0.006	0.001
BannLower	-0.043	-0.035	0.083	0.081	-	0.014*	0.013	0.009	0.017**	0.008	0.017*	0.016	0.008*
LoughComber	0.127*	0.004	0.022	0.055	0.043	-	-0.001	-0.004	-0.004	0.006	-0.004	0.002	-0.008
Larne Lough	-0.043	0.010	0.161**	0.140*	-0.048	0.127*	-	0.003	0.004	0.004	0.006	0.005	0.000
Boretree	-0.006	-0.014	0.077	0.093*	-0.069	0.020	-0.017	-	0.003	-0.003	0.005	0.005	-0.005
GlynnLagoon	0.002	-0.028	0.089*	0.069	-0.034	0.035	-0.017	-0.011	-	0.004	0.005	0.001	-0.004
Denmark	0.062*	-0.007	0.058*	0.072*	0.010	-0.013	0.037	0.007	-0.016	-	0.002	-0.008	0.004
Finland	-0.002	-0.015	0.090*	0.088*	-0.034	0.047	-0.032	-0.011	-0.024	-0.011	-	-0.002	-0.003
Germany	-0.046	-0.008	0.150**	0.096	-0.048	0.103*	-0.046	-0.017	-0.008	0.042	-0.014	-	-0.003
Portugal	-0.009	-0.035	0.089*	0.043	-0.035	0.019	-0.012	-0.018	-0.028	-0.004	-0.019	-0.030	-

Pairwise mismatch comparisons for both type of markers Pairwise locations differentiation based on haplotype frequencies for mtDNA (below diagonal) and genotype frequencies for five microsatellite loci, (above diagonal) after removal of loci Aan02. Aan02 was removed because this locus did not follow Hardy Weinberg equilibrium. Significant comparisons are highlighted in bold (* $p<0.05$, ** $p<0.01$ and *** $p<0.001$).

Table S7 – Test for neutral evolution of the mitochondrial marker
McDonald & Kreitman test

	First site	Second site	Third site
<i>Synonymous substitutions</i>			
fixed difference between species	0	0	4
Polymorphic sites	0	10	24
<i>Nonsynonymous substitutions</i>			
fixed differences between species	4	4	0
Polymorphic sites	33	27	14
Fisher exact test p-value	>0.05	>0.05	>0.05

McDonald & Kreitman test assuming all possible positions for a coding region to start, in the given ND5 fragment between the European and the American eels: The McDonald & Kreitman [S17] test assumes that a similar ratio of non-synonymous to synonymous substitutions between closely related taxa within the same coding region is an evidence of neutrality. As such, eight sequences of *Anguilla rostrata* were added to the data set in order to check if the amplified ND5 region was under any sort of selection. The test was performed after sequential assignment of the three possible coding positions for the first site before assigning a coding region to our fragment.

Supplemental experimental procedures

Text S1

The 355bp ND5 mtDNA fragment was amplified in a reaction containing 1ul 10x Buffer, 1ul (10mM) dNTPs, 1ul [5 pmol/ul] each primer (Forward: GCCCCTCAGAATGATATTGTCTCA reverse: AATAGTTTATCCRTTGGTCTTAGG) [S16], 0.1 Taq, 4.9 μ l H₂O and 1 μ l template. PCR conditions were as follow: 3min at 95 °C, 35sec at 95 °C, 40sec at 59 °C, 1sec at 72°C for 30cycles, 4min at 72°C. PCR products were cleaned with Exonuclease and FastAP (Fermentas) and directly sequenced from the reverse direction.

The nuclear loci were amplified in duplex (Aan01 and Aa02) [S16] and 3 multiplexes: 1 - B09, I14, M23, Aan03; 2- CT77,CT87, CA55,CA58,CA68, AjTR-37 ; 3- CT82, CT76, CT89, CT59, CA80, CT53 [S17-S19]. Duplex was performed in the following reaction conditions: 1 μ l 10x Buffer, 0.5 μ l (10mM) dNTPs, 1 μ l each primer 5pmol/ul, 0.05ul Taq 3.45 and 1ul DNA template. PCR conditions were the following: 3min at 95 °C, 35sec at 95 °C, 30 sec at 61 °C, 40 sec at 72°C for 30 cycles, 5min 72 °C; multiplex reaction was performed with QIAGEN© Multiplex PCR kit, following manufacturer instructions. Genotyping was then performed on a ABI ® 3100 Genetic Analyzer

Molecular and phylogenetic analyses using mtDNA were performed using the software DnaSP v5.10.01 [S20], NETWORK v4.6.1.0 [S8], and MEGA [S6]. To estimate the strength of neutral evolution, we added eight sequences of the ND5 fragment from *Anguilla rostrata* to the data set and performed a McDonald and Kreitman test [S21]. Departures from mutation/drift equilibrium were tested by means of Tajima's D test [S22]. Pairwise population differentiation comparisons were performed in Arlequin v3.5 [S23], by calculating Wright's index (F_{ST}) based on haplotype frequencies (10.000 permutations). Patterns of isolation by distance were investigated using $F_{ST}/(1-F_{ST})$ and log transformed geographic distances by the means of Mantel tests run on IBDWebService [S24]. F_{ST} were chosen because they can be combined with oceanic modeling outcomes to test for multiple scenarios of genetic structure in the spawning ground.

Microsatellites were called using GeneMarker® software. Molecular indices were calculated in MStoolkit [S25] and GENETIX v4.5.02 [S26]. Pairwise population differentiation comparisons were performed in Arlequin v3.5 [S23] by calculating Wright's index (F_{ST}) based on allele frequencies (10.000 permutations). Patterns of isolation by distance were investigated using $F_{ST}/(1-F_{ST})$ and log transformed geographic distances by the means of Mantel Mantel tests run on IBD Web Service [S24].

Supplemental references:

- S1. Jenkins, A.D., and Bye, J.A.T. (2006). Some aspects of the work of V.W. Ekman.
- S2. Friedland, K.D., Miller, M.J., and Knights, B. (2007). Oceanic changes in the Sargasso Sea and declines in recruitment of the European eel. *ICES Journal of Marine Science: Journal du Conseil* 64, 519-530.
- S3. McCleave, J.D., Kleckner, R.C. & Castonguay, M. (1987). Reproductive sympatry of American and European eels and implications for migration and taxonomy. In *American Fisheries Society Symposium Volume 1*. pp. 286-297.
- S4. Castonguay, M., and McCleave, J.D. (1987). Vertical distributions, diel and ontogenetic vertical migrations and net avoidance of leptocephali of anguilla and other common species in the Sargasso Sea *Journal of Plankton Research* 9, 195-214.
- S5. Bonhommeau, S., Chassot, E., and Rivot, E. (2008). Fluctuations in European eel (*Anguilla anguilla*) recruitment resulting from environmental changes in the Sargasso Sea. *Fisheries Oceanography* 17, 32-44.
- S6. Tamura, K., Dudley, J., Nei, M., and Kumar, S. (2007). MEGA4: Molecular Evolutionary Genetics Analysis (MEGA) Software Version 4.0. *Molecular Biology and Evolution* 24, 1596-1599.
- S7. Tamura, K., Subramanian, S., and Kumar, S. (2004). Temporal Patterns of Fruit Fly (*Drosophila*) Evolution Revealed by Mutation Clocks. *Molecular Biology and Evolution* 21, 36-44.
- S8. Bandelt, H.J., Forster, P., and Röhl, A. (1999). Median-joining networks for inferring intraspecific phylogenies. *Molecular Biology and Evolution* 16, 37-48.
- S9. von der Heyden, S., Lipinski, M.R., and Matthee, C.A. (2007). Mitochondrial DNA analyses of the Cape hakes reveal an expanding, panmictic population for *Merluccius capensis* and population structuring for mature fish in *Merluccius paradoxus*. *Molecular Phylogenetics and Evolution* 42, 517-527.
- S10. McCarthy, G., Frajka-Williams, E., Johns, W.E., Baringer, M.O., Meinen, C.S., Bryden, H.L., Rayner, D., Ducez, A., Roberts, C., and Cunningham, S.A. (2012). Observed interannual variability of the Atlantic meridional overturning circulation at 26.5°N. *Geophysical Research Letters* 39, L19609.
- S11. Bleck, R. (2002). An oceanic general circulation model framed in hybrid isopycnic-Cartesian coordinates. *Ocean Modelling* 4, 55-88.
- S12. Madec, G. (2008). NEMO = the OPA9 ocean engine. I.P.S. Laplace, ed. (France).
- S13. Fossette, S., Putman, N.F., Lohmann, K.J., Marsh, R., and Hays, G.C. (2012). A biologist's guide to assessing ocean currents: a review. *Marine Ecology Progress Series* 457, 285-301.
- S14. Rousset, F.o. (1997). Genetic Differentiation and Estimation of Gene Flow from F-Statistics Under Isolation by Distance. *Genetics* 145, 1219-1228.
- S15. Ptak, S.E., and Przeworski, M. (2002). Evidence for population growth in humans is confounded by fine-scale population structure. *Trends in Genetics* 18, 559-563.
- S16. Daemen, E.D., Cross, T.C., Ollevier, F.O., and Volckaert, F.V. (2001). Analysis of the genetic structure of European eel (Anguilla anguilla) using microsatellite DNA and mtDNA markers. *Marine Biology* 139, 755-764.
- S17. Pujolar, J.M., De Leo, G.A., Ciccotti, E., and Zane, L. (2009). Genetic composition of Atlantic and Mediterranean recruits of European eel *Anguilla anguilla* based on EST-linked microsatellite loci. *Journal of Fish Biology* 74, 2034-2046.
- S18. Pujolar, J.M., Maes, G.E., Van Houdt, J.K.J., and Zane, L. (2009). Isolation and characterization of expressed sequence tag-linked microsatellite loci for the European eel (*Anguilla anguilla*). *Molecular Ecology Resources* 9, 233-235.
- S19. Wielgoss, S., Wirth, T., and Meyer, A. (2008). Isolation and characterization of 12 dinucleotide microsatellites in the European eel, *Anguilla anguilla* L., and tests of amplification in other species of eels. *Molecular Ecology Resources* 8, 1382-1385.

- S20. *Librado, P., and Rozas, J. (2009). DnaSP v5: a software for comprehensive analysis of DNA polymorphism data. Bioinformatics 25, 1451-1452.*
- S21. *McDonald, J.H., and Kreitman, M. (1991). Adaptive protein evolution at the Adh locus in Drosophila. Nature 351, 652-654.*
- S22. *Tajima, F. (1989). Statistical method for testing the neutral mutation hypothesis by DNA polymorphism. Genetics 123, 585-595.*
- S23. *Excoffier, L., and Lischer, H.E.L. (2009). Arlequin suite ver 3.5: a new series of programs to perform population genetics analyses under Linux and Windows. Molecular Ecology Resources 10, 564-567.*
- S24. *Jensen, J., Bohonak, A., and Kelley, S. (2005). Isolation by distance, web service. BMC Genetics 6, 13.*
- S25. *Park, S.D.E. (2001). Trypanotolerance in West African Cattle and the Population Genetic Effects of Selection. Volume Doctor of Philosophy. (Dublin: University of Dublin).*
- S26. *Belkhir K, B.P., Goudet J, Chikhi L, Bonhomme F (1999). Genetix, logiciel sous Windows TM pour la genetique des populations., U.d.M. Laboratoire Genome et Populations, ed. (France).*